ABSTRACT

Title of Thesis: DISPENSER PHOTOCATHODES FOR ACCELERATOR APPLICATIONS

Degree candidate: Matt Virgo

Degree and year: Master of Science, 2002

Thesis directed by: Professor Patrick G. O'Shea
Department of Electrical Engineering

Over the past several years, RF photoinjectors have become the electron source of choice when high quality, intense beams are required. One of the fundamental decisions that must be made in the design of any photoinjector is the choice of photocathode. Currently, no photocathode offers both high current capability and long lifetime. A cathode that meets both of these requirements would be useful in all situations, and it is necessary for military applications where frequent maintenance would be impractical. At the University of Maryland, an effort is currently underway to expand the concept of the thermionic dispenser cathode to photocathode applications. By constantly replenishing the emitting surface, such a cathode could function for extended periods of time without requiring human intervention. The first steps in this project are reported here. A photocathode test cell was developed, and a preliminary study of the characteristics of a scandate dispenser cathode was carried out.

DISPENSER PHOTOCATHODES FOR ACCELERATOR APPLICATIONS

by

Matt Virgo

Thesis submitted to the Faculty of the Graduate School of the
University of Maryland, College Park in partial fulfillment
of the requirements for the degree of
Master of Science
2002

Advisory Committee:

Professor Patrick G. O'Shea, Chair
Professor Jon Orloff
Professor Martin Reiser

ACKNOWLEDGEMENTS

This project would not have been possible without the contributions of Donald Feldman, Kevin Jensen, Patrick O'Shea, Jay Pyle, Bryan Quinn, Martin Reiser, and John Rodgers

TABLE OF CONTENTS

LIST OF TABLES

LIST OF FIGURES

Chapter 1

Introduction

1.1 Photocathodes for Accelerators

The photoelectric effect was first seen in experiments conducted by Hertz in the late nineteenth century. A theory was developed by Einstein, for which he was awarded the Nobel Prize in 1921. Since then, the field has been important to both science and technology. Scientifically, it played a central role in the development of quantum mechanics. From a technological perspective, an understanding of the photoelectric effect has made possible fast, sensitive optical detectors. More recently, photoemissive materials have been used as sources of high brightness electron beams, the topic of this thesis.

A photocathode based accelerator source is known as a photoinjector. Photoinjectors consist of an electron gun with a photocathode driven by a laser. The first photoinjector, which used a dc accelerating field, was developed at the Stanford Linear Accelerator Center in the 1970's as a source of polarized electrons for particle physics experiments. As described in Appendix B, a laser can also be used to produce perturbations on a thermionic pulse for beam physics studies.

Electron beam based coherent radiation sources, such as free electron lasers, re-

quire sources of intense, high quality beams. The search for such a source led to the development of the rf photoinjector at Los Alamos National Laboratory in the 1980's [1]. This device consists of a photocathode placed directly inside an rf accelerating structure, as shown in figure 1.1.

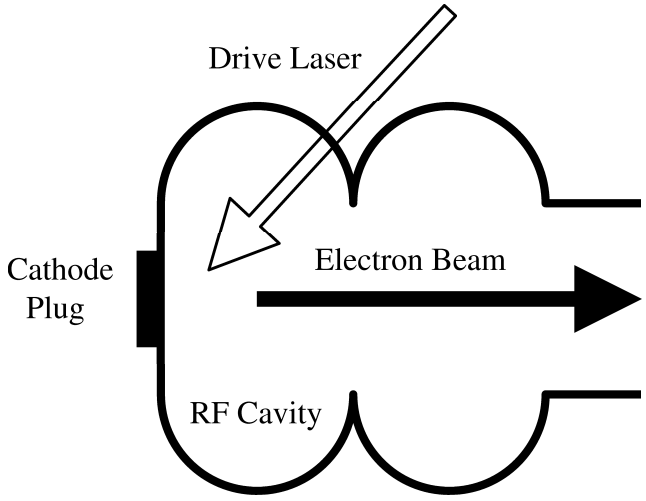

Figure 1.1: Components of a photoinjector

The rf photoinjector has several advantages over a conventional thermionic source [2]. Higher field strengths can be achieved in an rf structure, which means that more current can be drawn from the cathode. Also, the electrons are quickly accelerated to high energy where the beam is less susceptible to quality degradation. Furthermore, in a thermionic gun, the beam's temporal profile is determined by the accelerating field, and its spatial distribution is controlled by the cathode geometry. In a photoinjector, the current distribution is determined by the drive laser, so the electron pulse can be shaped with greater freedom.

The component of the photoinjector most directly tied to the cathode is the drive laser. The electron pulse must fill a small fraction of the rf phase. Otherwise, the accelerated electrons will have a large spread in longitudinal velocities, so the pulse

will stretch. In practice, a laser pulse of no more than several picoseconds must be used. This time structure is provided by mode locked YLF or Ti:SAF oscillators. The laser beam must then be amplified to produce the necessary energy. Photocathodes used in rf guns usually require visible or ultraviolet light, so frequency converting crystals are used to obtain shorter wavelengths. Unfortunately, a significant amount of energy is lost in the conversion process. Also, harmonic generation is nonlinear with laser intensity, so any power fluctuation on the input is exacerbated on the output. Furthermore, higher frequency light is more likely to damage the optics. Therefore, it is desirable to find new cathode materials that can operate at longer wavelengths.

There is an effort underway to develop free electron lasers capable of generating megawatts of average power. Design studies have determined that such a machine would require 1-nC electron bunches at a 1-GHz repetition rate. With a current cathode (Cs_2Te), the drive laser would need to produce several hundred watts of ultraviolet light, again at 1 GHz. No laser can deliver that pulse format, so better cathodes must be engineered.

When evaluating a photocathode, the following characteristics must be considered [3]:

Threshold wavelength Photons need to have enough energy to eject electrons from the material. A shorter threshold wavelength requires a more complicated, higher power drive laser.

Quantum efficiency The quantum efficiency of a cathode is the fraction of incident photons that produce photoelectrons. A lower quantum efficiency requires a higher power laser.

Promptness The electron pulse leaving a photocathode will be longer than the photon

pulse that generates it. If the increase is significant, the material will not make a suitable emitter.

Lifetime In the harsh operating environment of an rf gun, some cathodes last only hours. Others may last many months.

The two broadest categories for photoemitters are metals and semiconductors. Photocathodes within those categories share a set of common traits, which will be described in detail below.

1.2 Theory of Photoemission

1.2.1 The Three Step Model

A three step model has been developed to describe the process of photoemission from solids [4]. The first step is absorption of light into the solid. The second step is transport of electrons to the surface. The final step is escaping the surface barrier. This theory makes many assumptions which may not be obviously justifiable, but it accurately explains the behavior of a broad range of photoemissive materials. A more sophisticated analysis is presented in [5].

Step one in the three step model is the absorption of the photons into the material. Materials with a high optical absorption coefficient are potentially very good photoemitters. Materials that are very reflective will be less efficient. It should be noted that the absorption coefficient often increases substantially at shorter wavelengths.

The second step is the path of the electrons to the surface. If they undergo electron-electron scattering, they will loose energy, which reduces their chances of reaching the vacuum. Electron-lattice scattering also reduces the electron's energy, but the energy

loss per collision is much smaller than the total energy of the electron, so the effect less pronounced.

The final step is the penetration of the surface barrier. The surface barrier measures the distance from the highest densely filled states to the vacuum level. The photon energy needed to excite electrons to the vacuum level can range from infrared to ultraviolet.

1.2.2 The Schottky Effect

One aspect of the emission process that is particularly relevant in rf guns is the Schottky effect [6]. As the electric field at the surface of the cathode is increased, the energy that an electron needs to escape to the vacuum is decreased. The amount by which the work function is lowered is given by

$$\Delta\phi = \sqrt{\frac{eE}{4\pi\epsilon_0}}$$

where e is the electron's charge and E is the applied electric field. For instance, a field of 1 MeV/m lowers the work function by .038 eV, and a field of 100 MeV/m lowers the work function by .38 eV. There is no simple relationship between quantum efficiency and work function, but the quantum efficiency often increases by several times when the field is increased from 1 MeV to 100 MeV. However, if the photon energy is already very close to the surface barrier when no field is applied, the Schottky effect can increase the quantum efficiency by orders of magnitude.

1.3 Properties of Photocathodes

As described above, the important features of photocathodes are threshold wavelength, quantum efficiency, promptness, and lifetime. These characteristics, particularly the

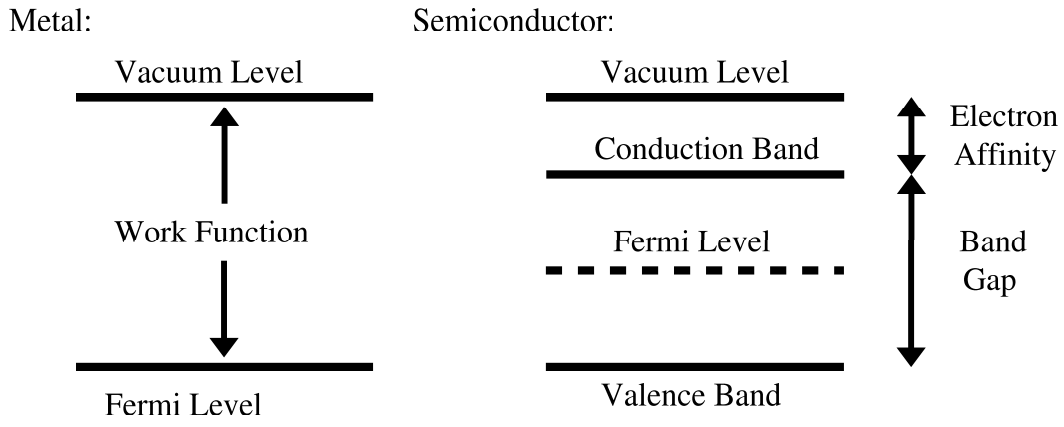

Figure 1.2: Model for photoemission in metals and semiconductors

first three, can be described in terms of the three step model.

1.3.1 Threshold Wavelength

The threshold wavelength for photoemission is primarily determined by the third step in the three step model, escaping the surface barrier. Figure 1.2 shows how this process differs between metals and semiconductors. In metals, it is the work function that measures the distance between the top of the valence band and the vacuum level. Photons must have an energy greater than the work function to stimulate photoemission.

The process is slightly more complicated in semiconductors. Few electrons are available in the conduction band, so electrons must be elevated from the valence band to the vacuum. Therefore, a photon must have an energy equivalent to the band gap E_G plus the electron affinity E_A (the distance from the bottom of the conduction band to the vacuum level) in order to free an electron from the material.

As the photon energy is raised passed the threshold for photoemission, the rise in electron yield is steep, but it is not instantaneous. The reason is that the parallel com-

ponent of an electron's momentum is conserved as it leaves the surface. Therefore, an electron must have enough total energy to both escape the surface barrier and satisfy conservation of momentum. By assuming a Fermi-Dirac distribution for electron velocities inside the material, the number of electrons that can escape the surface for photon energies near threshold can be determined.

Because the work function of a metal is the same as its surface barrier for photoemission, it is possible to find the work function of a metal by fitting the experimental data for quantum efficiency as a function of photon energy to the theoretical curve. This technique was developed by Fowler [7].

1.3.2 Quantum Efficiency

When comparing cathodes, quantum efficiency is the most commonly encountered figure of merit. It is helpful to put the quantum efficiency into a form that uses the units measured during experiments. If QE is the quantum efficiency, N_{Photon} is the number of incident photons, $N_{Electron}$ is the number of photoemitted electrons, E_{Laser} is the energy per pulse of the laser, Q_{Beam} is the charge in the electron beam, and $h\nu_{eV}$ is the photon energy in electron volts,

$$QE = \frac{N_{Photon}}{N_{Electron}} \tag{1.1}$$

$$E_{Laser} = (h\nu_{eV})(1.6 \times 10^{-19})\, N_{Photon}$$

$$Q_{Beam} = (1.6 \times 10^{-19})\, N_{Electron}$$

Inserting the second two equations into the first yields:

$$QE = \frac{E_{Laser}}{Q_{Beam}\, h\nu_{eV}} \tag{1.2}$$

The best photoemitters have quantum efficiencies of around .5. Photocathodes used in rf guns typically range in quantum efficiency from roughly .1 to 10^{-5}. The

first and second steps in the three step model primarily determine quantum efficiency. The effect of the first step is clear: only photons that are absorbed by the material can lead to photoemission.

The large variation in quantum efficiency from one material to the next is a result of the second step. In semiconductors, the band gap lies above the valence band, so little electron-electron scattering is allowed to take place. Electron-lattice scattering causes a minimal reduction in the electrons' energy, so they can escape from deep inside the material. By contrast, electrons in a metal undergo many collisions with other electrons on their path to the surface, so fewer electrons can escape.

In a semiconductor, if the band gap is small compared to the electron affinity, a photon may excite two electrons to the conduction band instead of elevating one to the vacuum level. As a result, the photon generates no photoelectrons. Materials with this property usually have a poor quantum yield. However, it is also possible for a single photon (in a metal or semiconductor) to excite two photons to the vacuum level. Therefore, a quantum efficiency greater than unity can be attained.

It is also possible for two photons, neither of which has energy greater than the surface barrier, to excite a single electron to the vacuum. From a practical standpoint, this effect requires power densities at the limits of what can currently be achieved, so it is rarely exploited in electron sources for accelerators.

1.3.3 Promptness

As described in the introduction, accelerators require electron bunches no more than several picoseconds long. The factor that determines the response time for a cathode is the depth to which photons penetrate the material. As described above, electrons exiting a metal cathode lose significant energy through scattering, so electrons generated

deeply within the emitter are unlikely to escape to the vacuum. Therefore, metals have a short response time. In semiconductors, the opposite is true, so they will have longer response times.

1.3.4 Lifetime

Cathode lifetime is primarily determined by the formation of surface films. Oxides are the most common contaminant. This problem is particularly pronounced in rf guns, where the requirements on the cavity geometry place restrictions on the design of the vacuum system. Typically, the vacuum will be on the order of 10^{-7} to 10^{-8} torr. In dc guns, ion back bombardment increases the reactivity of the cathode surface, which also accelerates poisoning. Damage from the drive laser is another factor that may limit lifetime.

1.4 Cathode Types

Photocathodes can be broken down into two broad categories: metals and semiconductors. Here, the traits shared by cathodes within those groups are discussed. Also, cesiated metal and negative electron affinity cathodes, are treated separately because of their practical importance.

1.4.1 Metals

Copper is the most common photocathode for accelerators. It is used because it is easy to prepare and has an indefinite lifetime. Copper cathodes require only machining, polishing, and cleaning before being installed. Also, they have a femtosecond response time, so they are prompt emitters. The down side is that copper has a quantum effi-

ciency of 1×10^{-5} to 1×10^{-4}, so lots of laser energy is needed to generated significant charge. Also, the work function of copper is over 4 eV, so an ultraviolet laser is needed. Magnesium has been used as an alternative to copper. It has similar properties, but its quantum efficiency is about 10 times greater.

1.4.2 Semiconductors

The first photocathode used in an rf gun was cesium potassium antimonide [1]. When new, these cathodes have the highest quantum efficiency currently attainable in an rf gun, over 5% with green light and over 10% with ultraviolet light. They also have a sub picosecond response time, so they are prompt. However, they only last one day in an accelerator. Cesium telluride is the most commonly used semiconductor cathode [8]. It requires an ultraviolet laser, but it has a relatively high quantum efficiency (greater than 1%), it is a prompt emitter, and it can last months.

1.4.3 Cesiated Metals

It has been found that metals such as tungsten, when coated with a thin layer of cesium, can have a work function lower than either tungsten or cesium. Conceptually, the cesium atoms give up electrons to the substrate, creating a dipole layer that reduces the surface barrier. A more accurate quantum mechanical theory has been developed [9]. These cathodes have few advantages over semiconductor cathodes, so they are not used in rf guns.

1.4.4 Negative Electron Affinity

Negative electron affinity (NEA) [10] cathodes have the highest quantum efficiencies. Exposing a p-type semiconductor to cesium and oxygen produces downward band bending at the surface that can reduce the electron affinity of the cathode below zero. Then, any electron that has enough energy to pass the band gap will be emitted from the material. Unfortunately, because electrons from far within the material can still be emitted, these cathodes have long response times. However, gallium arsenide is commonly used in dc photoinjectors as a polarized electron source. With the vacuum levels achievable in a dc gun (better than 10^{-11} torr), the lifetime of GaAs can be months, but it is highly susceptible to contamination at higher pressures.

1.5 Review of Current Photocathodes

Despite the relatively large number of photoemitters evaluated for use in accelerators, only a few are widely used. Table 1.1 lists the most common ones with their properties. In this section, their strengths and weaknesses are described.

Material	QE	Wavelength	Lifetime	Prompt?
K_2CsSb	10^{-1}	Green	Hours	yes
Cs_2Te	10^{-2}	UV	Weeks	yes
Mg	10^{-3}	UV	Months	yes
Cu	10^{-4}	UV	Months	yes
GaAs+Cs	10^{-1}	IR	Months	no

Table 1.1: Comparison of commonly used photocathodes

1.5.1 New Approaches

Currently, researchers are taking a number of approaches to improving photocathodes. At Vanderbilt, a tungsten tip illuminated with the fourth harmonic of YAG is being used to generate intense beams. Although the work function of tungsten is greater than the photon energy, the Schottky effect lowers the surface barrier enough to allow emission. At Los Alamos, silicon carbide infused with cesium will be studied. The photoemissive properties of niobium, which is used to make superconducting cavities, are being investigated at Brookhaven. At Cornell, researchers are attempting to achieve shorter pulses from NEA cathodes.

1.6 Dispenser Cathodes

1.6.1 Thermionic Mode

Dispenser cathodes are the electron source used in microwave tubes. In this device, a porous plug is impregnated with low work function material that flows to the surface when the cathode is heated. Because the emitting surface is continuously refreshed, the cathode can have a lifetime of years, and it is resistant to poisoning. Because of their importance in radar and communications, extensive effort has been invested in their optimization.

The standard dispenser cathode consists of a tungsten plug impregnated with barium oxide, calcium oxide, and aluminate [11]. The way the cathode operates is not fully understood. It is believed that the barium oxide reacts with the aluminate and tungsten to release barium when the cathode is heated. A film of barium and oxygen is then formed on the surface. Like a cesiated tungsten photocathode, this process induces a dipole layer that enhances the electric field, effectively reducing the work

function below that of pure barium. The calcium oxide is believed to regulate the rate at which barium diffuses to the surface. This device is known as the B cathode. It is further categorized by the ratio of barium oxide to calcium oxide to aluminate. Popular versions are the 5:3:2, the 4:1:1, and the 6:1:2.

Later, it was discovered that a thin (hundreds of nanometers) layer of a high work function metal such as osmium reduces the overall work function of the cathode. However, because this cathode relies on a surface film, it is more susceptible to damage. This is known as the type M.

As an alternative to a coating, it has been found that the addition of a small amount (2–7% by weight) of scandate to the impregnate also produces a work function below that of pure barium. In thermionic mode, this cathode can produce the highest current density of the standard cathodes. It is not commonly used, though, because the simpler B cathode generates enough current for most uses.

1.6.2 Photoemission

Barium itself has a work function of about 2.2 eV. The type B cathode has a work function of roughly 2 eV, and work functions reported for the type M and scandate cathodes range from 1.6–2.0 eV [12]. The commonly used metal photocathodes, copper and magnesium, have work functions of 4.4 eV and 4.0 eV, respectively. The second, third, and fourth harmonics of YAG have photon energies of 2.34 eV, 3.51 eV, and 4.68 eV. Therefore, although copper cathodes require the fourth harmonic, it should be possible to get photoemission from dispenser cathodes with the second and third harmonics. This was found to be true. It was shown that a B type cathode has a quantum efficiency of 2.5×10^{-5} at the second harmonic, 1×10^{-4} at the third harmonic, and 3.5×10^{-4} at the fourth harmonic [13]. Experiments at the University of Maryland

supported this result [14]; a quantum efficiency of 7.4×10^{-5} was found using a nitrogen laser, which is roughly equivalent to the third harmonic of YAG. In the original experiments, the cathode was also tested in an rf gun [15].

M type and scandate cathodes had not yet been tried. Because the work function of all of these cathodes is close to the second harmonic, a small decrease in work function could lead to a large increase in quantum efficiency. The first data for scandate cathodes is reported later in this document.

Chapter 2

Experimental Apparatus

2.1 Mechanical

The cathode test cell is constructed almost entirely from off-the-shelf 2.75-in conflat hardware. The vacuum is maintained with a 30-l/s ion pump and monitored with an ion gauge. In order to study the cathodes in a reasonably steady state, a vacuum on the order of 10^{-9} torr is required. This is accomplished with an overnight bakeout to 100 C.

A linear translation stage is used to adjust the anode-cathode distance. As shown in figure 2, the position of the anode is fixed relative to the table. As the bellows are extended, the whole cathode assembly is moved away from the system. This obviates the need for moving parts inside the vacuum, thus simplifying the system. The zero reference is set by moving the anode and cathode together until they trigger the continuity detector of a multimeter.

The cathode is electrically connected to the back flange, which is isolated from the rest of the system by a 2-in long ceramic gap rated for 15 kV. The different cathodes being studied have the same dimensions and are mounted the same way, so no modifications must be made in order to change the cathode. A copper cathode and dispenser

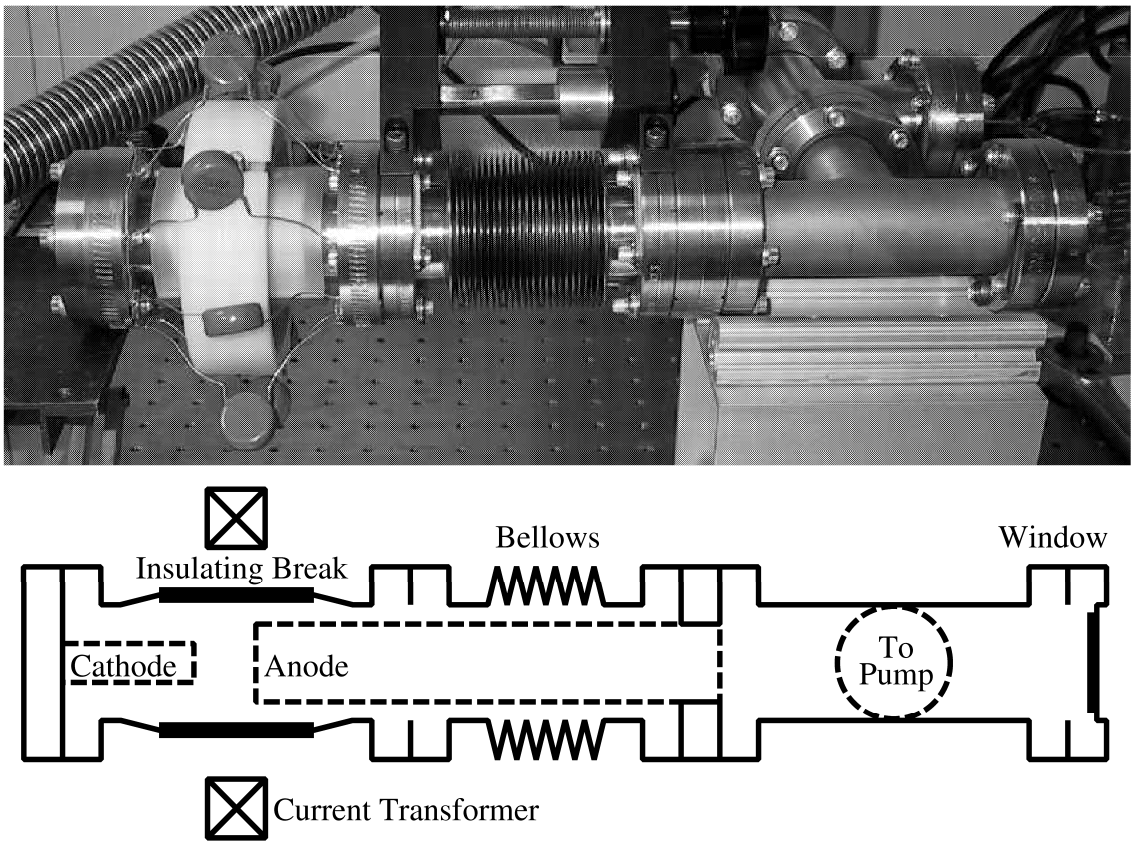

Figure 2.1: Layout of the photocathode test cell

cathode are shown in figure 2.2. In order to minimize the effect of field enhancement, it is desirable to have the smoothest possible cathode surface. The copper cathode was machined, sanded with 240, 400, and 600-grit sandpaper, and polished with 30-μm, 9-μm, and finally 3-μm silicon carbide polishing paper. The grooves that are visible in the figure are separated by approximately 50 μm, corresponding to the feature spacing of the 600-grit sandpaper. If another copper cathode is made, sandpaper of up to 1000-grit will be used before polishing. This should improve the cathode surface significantly.

The anode is made of a mesh so that the laser can be directed onto the cathode at normal incidence. The mesh, which is made of electroformed nickel, is stretched

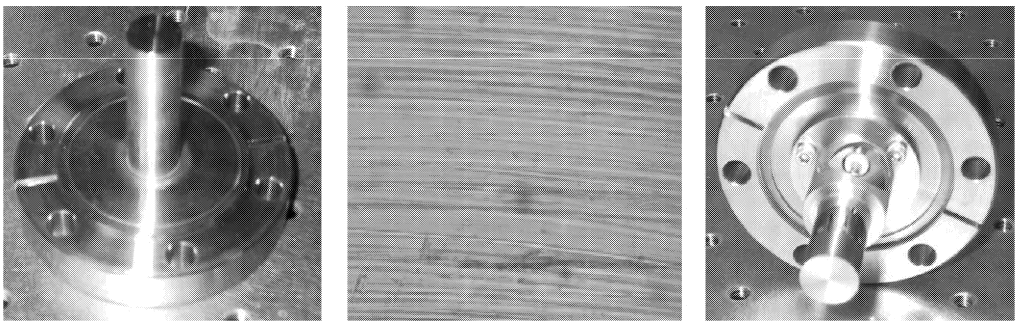

Figure 2.2: From left to right: Copper cathode, microscope image of the copper cathode, scandate cathode

across a 1-in aluminum ring. The wire width is 14.7 μm, and the holes are 112 μm across. It provides 78% transmission. The anode is connected to an aluminum tube which carries the current back to ground. Most of the wall of the tube has been removed to improve its vacuum performance. The tube is supported by a double sided flange. These components are shown in figure 2.3.

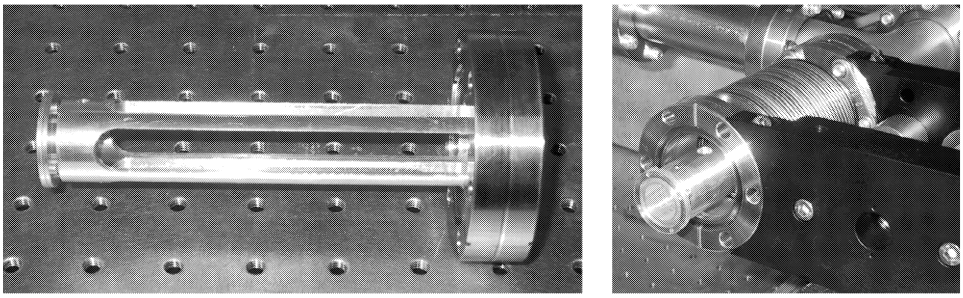

Figure 2.3: Picture of the anode and anode support

2.2 Electronics

A Glassman series EH 15 kV-dc power supply is used to generate the extraction voltage. In order to prevent an accidental arc from destroying the grid, a 50-MΩ resistor is

inserted between the power supply and the diode. At 15 kV, this limits the dc current passing through the grid to .4 mA.

In order to prevent voltage droop during the pulse, an external capacitance is added between the cathode and the anode. Experimentally, it was found that the maximum (space charge limited) charge that could be drawn was about 5 nC. Assuming a slightly higher charge of 10 nC and a maximum allowable droop of 10 V at 10 kV (.1%), 1 nC of capacitance is required. High performance NPO ceramic capacitors are used.

2.3 Laser

Because of the rf accelerating field, photoinjector drive lasers produce picosecond pulses using mode locked semiconductor lasers. The test cell uses a dc field, so extremely short pulses are not required. A Q-switched YAG provides high energy, nanosecond pulses at the same wavelengths used with rf guns. The model is the Continuum Minilite II. It provides 50-mJ pulses of 1064-nm light at 10 Hz. The FWHM pulse width is 6 ns. Nonlinear crystals generate the second (532 nm), third (355 nm), and fourth harmonics (266 nm). The corresponding pulse energies are 25 mJ, 8 mJ, and 4 mJ, respectively. During the harmonic generation process, the pulse is shortened to 4 ns FWHM. The laser produces a 3-mm beam with a 3 mrad divergence.

A telescope is used to adjust the size of the spot on the cathode. Two mirrors are then used to adjust the position and angle of the beam so that it can be positioned on the cathode. Figure 2.4 shows the optical layout. Because glass windows severely attenuate ultraviolet light, a quartz window is needed to transmit the third and fourth harmonics. 3.5% of the incident light reflects off each surface of the window, so it has a 93% transmission coefficient. A final component that must be taken into account

when considering the optics is the anode grid. It is 78% transmissive. When combined with the effect of the window, only 72.5% of the light incident on the window reaches the cathode.

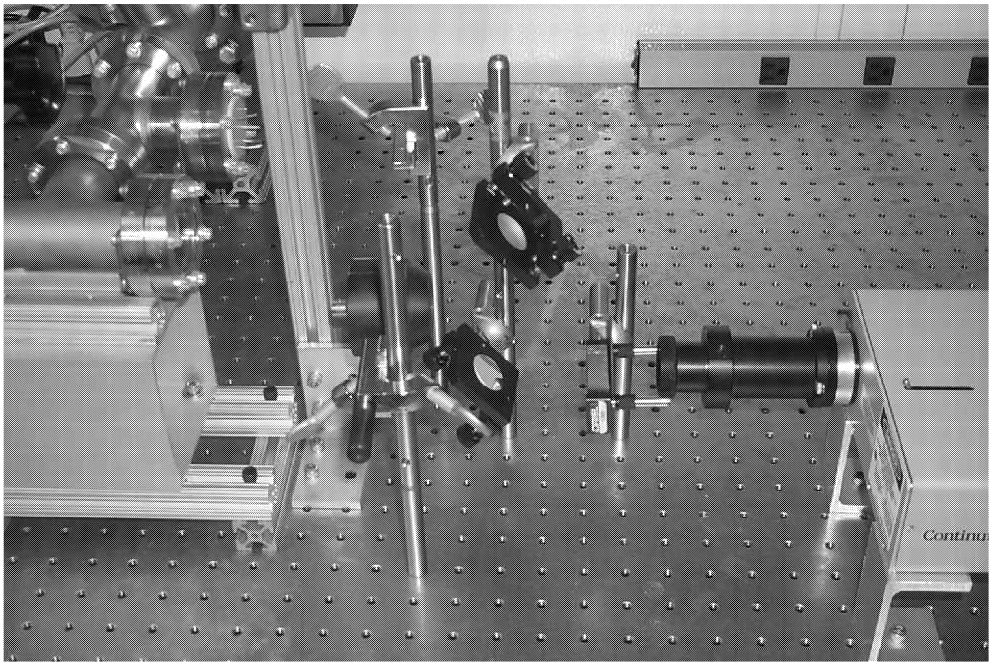

Figure 2.4: Optical components of the test cell

2.4 Diagnostics

The pulses used in the experiment are generally around 5 ns FWHM with a 2-ns rise time. Also, because of space charge effects, the electron beam may develop features of sub-nanosecond width. In order to characterize the pulses, a range of fast diagnostics are needed.

A LeCroy model LC564A 1-GHz oscilloscope is used. This model has a single shot sampling rate of 2 GS/s. It can resolve a rise time of 500 ps. Several of the scope's built in functions were used during the course of the experiments. Averaging mode was

used to reduce the effects of random noise resulting from shot to shot fluctuations of the laser, circuit oscillations, and pickup from the current transformer. Integration was used to determine the total pulse charge from the current trace. The amplitude and pulse width functions were also used.

The most important diagnostic for these experiments is a Bergoz model FCT-055-20:1 current transformer. The core is constructed from a CoFe/NiFe alloy, and the winding has 20 turns. It has a 2-GHz bandwidth and a 200-ps rise time. The sensitivity is 1.25 V/A.

The pulse energy is measured with a Spectra-Physics pyroelectric energy meter. It has a sensitivity of 6 mV/mJ. When attenuators are used to reduce the pulse energy below .5 mJ, the LeCroy no longer has sufficient sensitivity to measure the signal. For these measurements, a Tektronix model 7844 oscilloscope is used. It can measure microvolt signals. Laser pulse shapes are obtained with an Antel AR-S2 fast photodiode. It has a rise time of 35 ps, and it can measure a pulse of 65 ps FWHM.

2.5 Dispenser Cathode

Two identical 3:1:1 scandate dispenser cathodes were purchased from Spectra-Mat, Inc. The ratio of scandate to the other impregnates is proprietary, but it is on the order of a few percent. The cathode diameter is .5 in. It was shipped in nitrogen, but exposure to air for periods of several days does not cause permanent damage.

2.5.1 Heater

The temperature of the dispenser cathode is controlled by a molybdenum filament contained in the cathode body. A feedthrough on the back of the cathode flange is used

to supply the heater voltage. An isolation transformer allows the heater to be run when the cathode is floated at high voltage. An optical pyrometer is used to measure the temperature when the cathode becomes visible at around 700 C. Lower temperatures can be measured accurately by comparing the resistance of the heater element with the reference values for molybdenum.

2.5.2 Activation

Before they are used, dispenser cathodes must be activated. During the activation process, an initial layer of barium is formed on the cathode surface. Also, water that has been absorbed into the cathode must be driven off. If the cathode is heated too quickly, the water forms compounds that reduce emission and damage the cathode surface. Therefore, the cathode is slowly heated to a point beyond its normal operating temperature and is held it at that temperature for a short period of time.

Because barium is highly reactive, contaminants from the system may become trapped on the cathode surface. To minimize this effect, the system temperature must be kept below that of the cathode. This means that it is not possible to bake the system before activation. Also, the pressure at the cathode must be kept below 1×10^{-6} torr at all times.

Initially, the base system pressure was high and small increases in cathode temperature released large amounts of water, so the temperature was increased slowly. When the pressure leveled off, indicating that most of the water had been removed, the system was baked to 50 C for 10 hours. Then, the cathode temperature was increased in larger intervals until it became barely visible (600–700 C). At that point, the system was baked to 150 C for 10 hours. From there, the temperature was measured with a pyrometer. The temperature was raised by roughly 40 C each half hour to 1190 C. That

temperature was held for 1 hour, then the temperature was lowered to 900 C, which is the operating temperature for this cathode when it is used in thermionic mode.

Chapter 3

Results

This chapter is divided into two parts. In the first part, the performance of the cathode test cell is determined. In the second part, measurements are made on a copper cathode, and then the photoemissive properties of a scandate dispenser cathode are reported.

3.1 Quantum Efficiency Measurements

3.1.1 Characteristics of the Diagnostics

The pulse shape from a Q-switched laser should be approximately Gaussian. In figure 3.1, a 30 shot average of the signal from the photodiode is plotted together with a Gaussian curve. The extended tail on the detector signal is not expected, and it does not show up on the electron pulse, so it is most likely a characteristic of the detector. The width of the laser pulse is seen to be about 5 ns FWHM. Figure 3.2 shows the current pulse from the Bergoz coil when averaged over 30 shots. For comparison, the Gaussian fit to the laser pulse is also displayed. Here, it appears that the fall time of the current pulse is shorter than its rise time, however, the falling edge overlaps with ringing in the circuit, which may make the slope look steeper than it is.

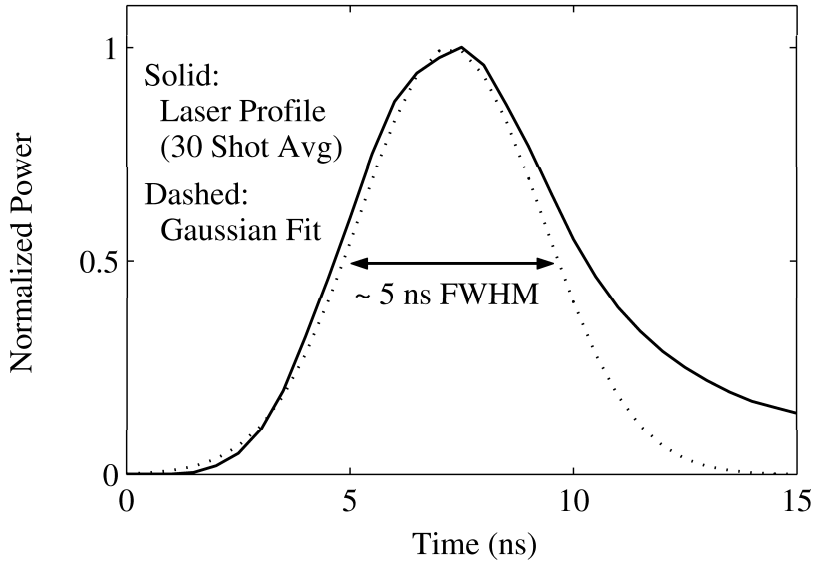

Figure 3.1: Laser profile measured with photodiode compared with Gaussian fit

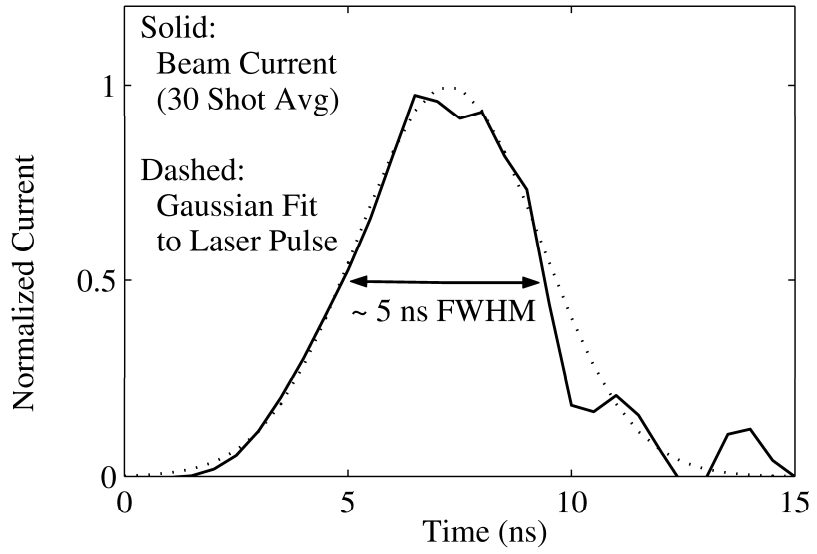

Figure 3.2: Beam profile compared with a Gaussian fit to the laser pulse

3.1.2 Space Charge Effects

For low currents, nearly all of the electrons that reach the vacuum level are collected at the anode. When the charge density in the anode-cathode region becomes too great, a

fraction of the charge is reflected back to the cathode. A more detailed discussion can be found in Appendix A. When this occurs, the measured quantum efficiency will be artificially low. Figure 3.3 shows the quantitative relationship between extraction field and total charge drawn. Figure 3.4 demonstrates how the current pulse is affected by

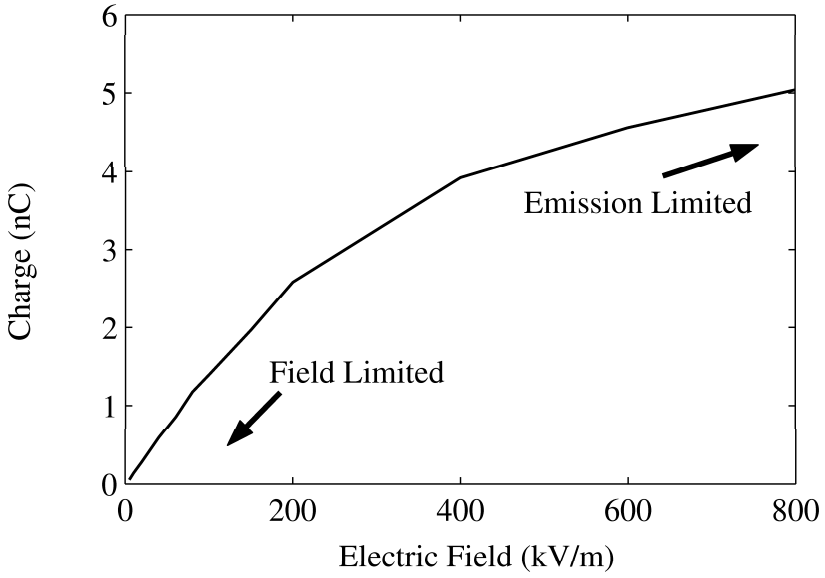

Figure 3.3: Reduction of measured charge due to space charge

strong space charge. In certain circumstances, an excess of charge in the gap can lead to the formation of instabilities [16]. In order to be confident that the full photocurrent is being measured, the extraction voltage is scanned over an order of magnitude. The laser energy is then attenuated until source limited operation is obtained.

3.2 Copper

In order to characterize the test cell, a copper cathode was used. Copper has a long lifetime, so its properties do not change much during the course of the experiments. Also, the behavior of copper is well known, so it makes a good benchmark. The work

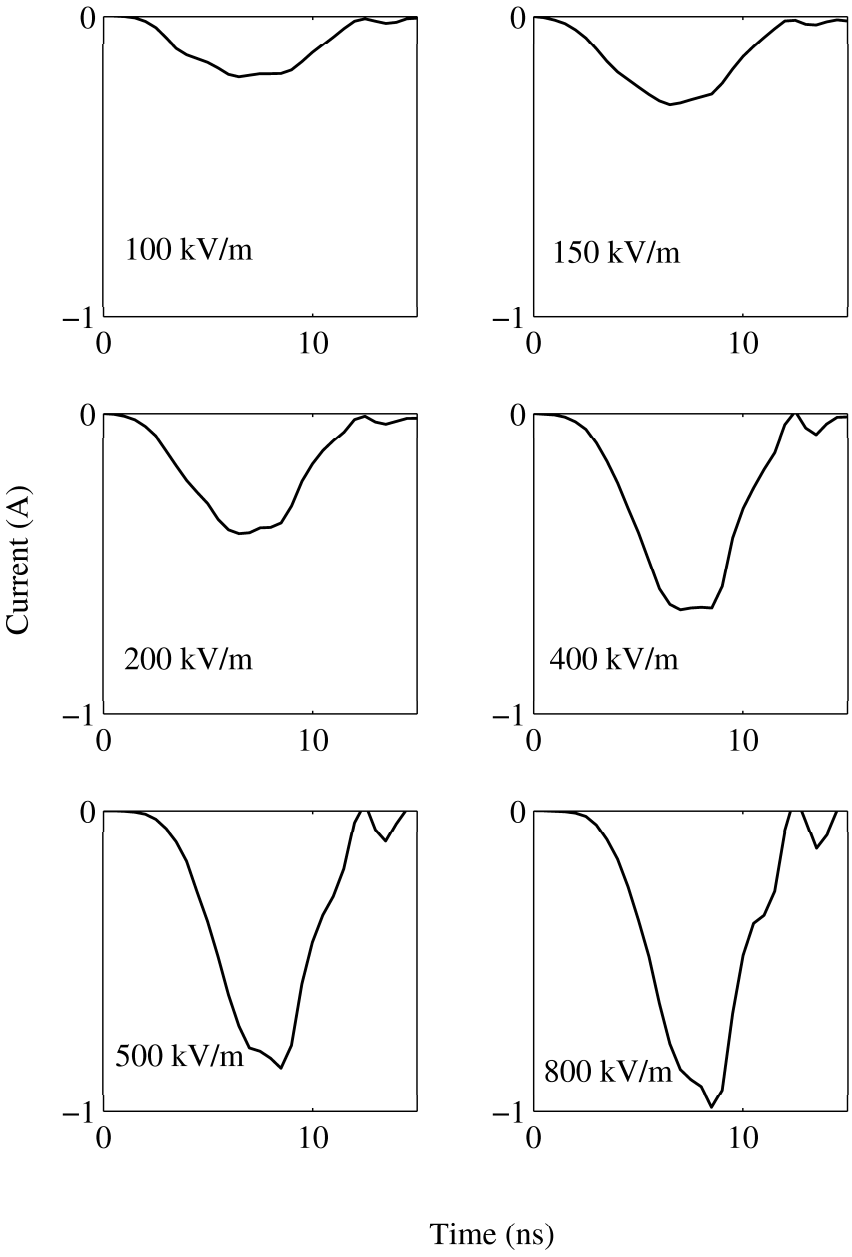

Figure 3.4: Effect of space charge on pulse structure

function of copper is about 4.5 eV, so photoemission is only observed at the fourth harmonic.

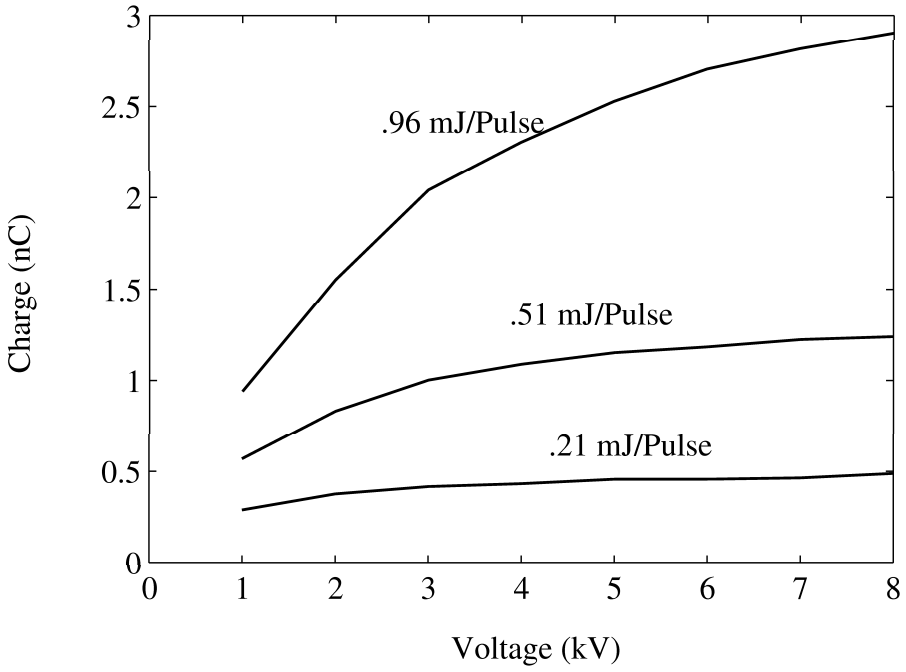

Figure 3.5: Diode current as a function of extraction potential for the copper cathode

Figure 3.5 shows traces of photocurrent in terms of extraction voltage. For these measurements, the anode-cathode gap is set to 5 mm. When the highest laser pulse energy is used, the emission is not entirely source limited, even for the largest extraction voltage. Using the data from the low laser energy trace, a .2-mJ laser pulse has generated 480 pC of charge. 266-nm light corresponds to a photon energy of 4.68 eV. From equation 1.2, the quantum efficiency is

$$QE_{Copper} \approx \frac{(480 \times 10^{-12})(4.68)}{.2 \times 10^{-3}} \approx 1 \times 10^{-5}$$

3.3 Dispenser Cathode

3.3.1 Thermionic Emission

The barium layer on the surface of the dispenser cathode acts as a getter. As contaminants accumulate, the quantum efficiency falls. Before measurements are made, the cathode must be heated so that a fresh layer is formed. The minimum temperature and times that are necessary have not yet been determined, but heating the cathode to 900 C for one hour is sufficient. Photoemission can not be measured at those temperatures because the thermionic emission would be significant. Thermionic emission is plotted against cathode temperature in figure 3.6. The cathode must be run at under 350 C to eliminate thermionic emission completely.

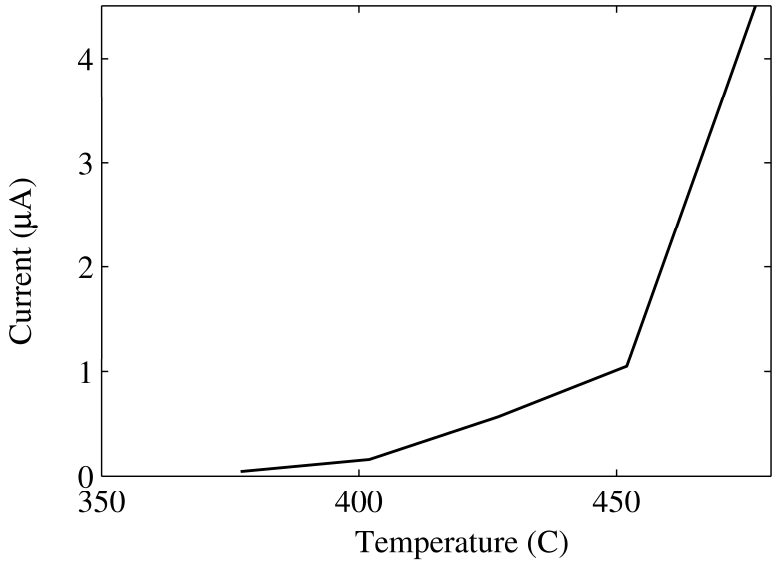

Figure 3.6: Thermionic current as a function of cathode temperature for the dispenser cathode

3.3.2 Fourth Harmonic

Figure 3.7 shows the cathode lifetime with 266-nm light under varying conditions. The origin of the time axis is when the heater voltage was reduced. Measurements are begun when the temperature has fallen enough that there will be no thermionic current. If any thermionic current occurs, electron bombardment of the surfaces inside the system releases particles, raising the pressure and reducing the cathode's quantum efficiency. As measurements are made, the quantum efficiency drops steeply at first, then levels off to a relatively stable value, even if the cathode is left overnight. At this point, a less reactive, higher work function contamination layer has formed. Running the cathode warm, but below the the threshold for thermionic emission, can slow the rate at which quantum efficiency falls and leads to a higher final value.

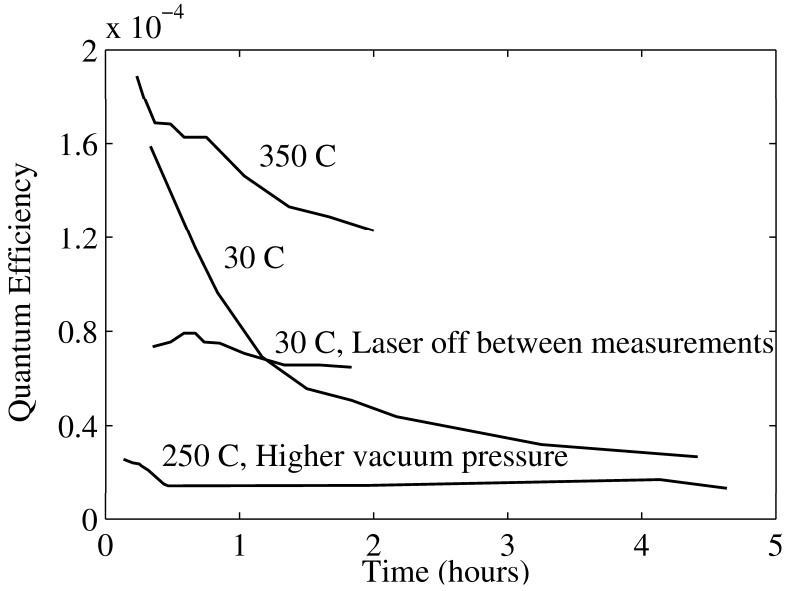

Figure 3.7: Dispenser cathode lifetime using 266-nm light

By running the laser in single shot mode, it was found that the efficiency drops roughly in half after the first laser pulse. This indicates that even small amounts of

ultraviolet light releases contaminants from the grid and other surfaces in very large quantities. The highest quantum efficiency obtained for a single shot has been 8×10^{-4}. By gaining a better understanding of the poisoning process, it may be possible to maintain this value over longer periods of time.

As described above, running the laser can instantly reduce the quantum efficiency. There is also a long term consequence. When the laser is run continuously between measurements, the system pressure rises about 50% above its value when the laser is only run for brief intervals. This effect is seen in the second plot from the bottom. Although the initial quantum efficiency is lower, the rate of decay is slower in this case. In some instances, though, shining the laser on the cathode can have a beneficial effect. If appreciable degradation has already occurred, the laser can knock contaminants from the cathode at a greater rate than new particles arrive. In this case, the light has a cleaning effect.

Figure 3.8 shows charge as a function of extraction field for the dispenser cathode with 266-nm light. This data was taken roughly 30 minutes after the cathode temperature was reduced. The quantum efficiency has already dropped from its peak value, but it was stable to within 10% during these measurements. The two low current curves indicate a quantum efficiency of 2.25×10^{-4}.

3.3.3 Third Harmonic

Theoretically, conversion to the third harmonic could be as efficient as conversion to the second harmonic. In actual lasers, however, the efficiency is closer to that of the fourth harmonic. Still, if the quantum efficiency of a cathode is similar at the third and fourth harmonics, it would be advantageous to operate at the lower one.

The quantum efficiency at the third harmonic is plotted as a function of time for

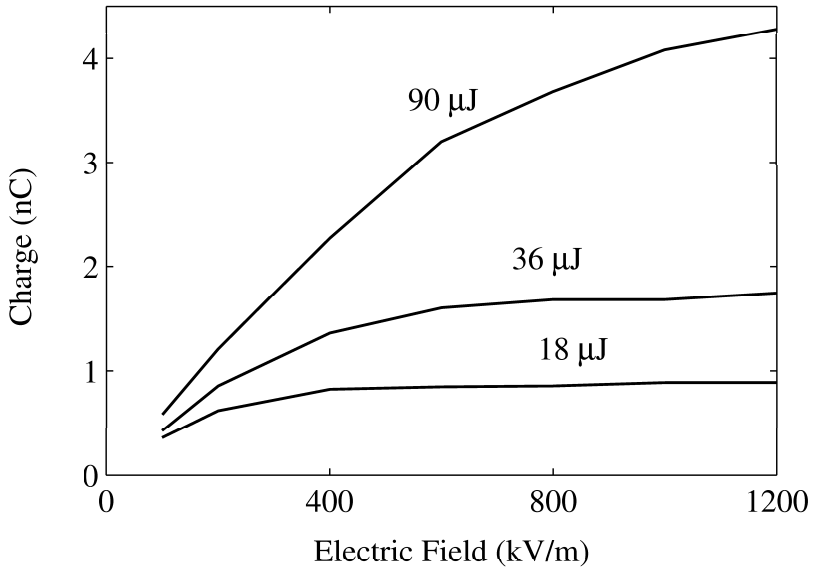

Figure 3.8: Charge related to extraction field for three laser energies with 266-nm light

three runs in figure 3.9. For this wavelength, the small increase in pressure from constantly running the laser has a more pronounced effect than it did at the fourth harmonic. This is because the high work function contamination layer pushes the threshold for photoemission to shorter wavelengths. At the fourth harmonic, there is still enough photon energy to overcome the barrier, but this is no longer the case at the third harmonic. Again, running the cathode at an elevated temperature is seen to hold the cathode at a higher quantum efficiency. A reproducible value of 1.7×10^{-4} has been observed.

3.3.4 Second Harmonic

Figure 3.10 shows quantum efficiency data with the second harmonic. Conversion to this wavelength can be very efficient, for instance 50% with the laser used here. As with the third harmonic, photoemission at the second harmonic is severely reduced if the laser is always on. A quantum efficiency of 6.2×10^{-5} is the best recorded so far.

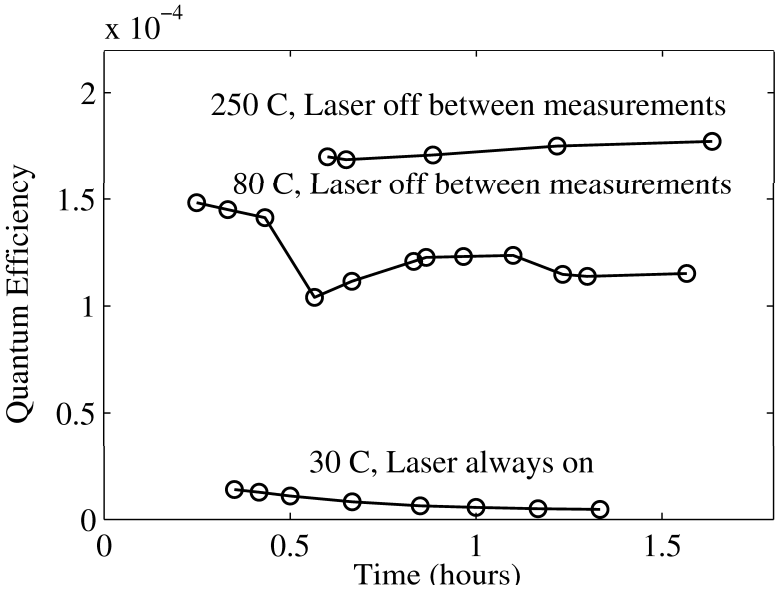

Figure 3.9: Quantum efficiency of the dispenser cathode with 355-nm light

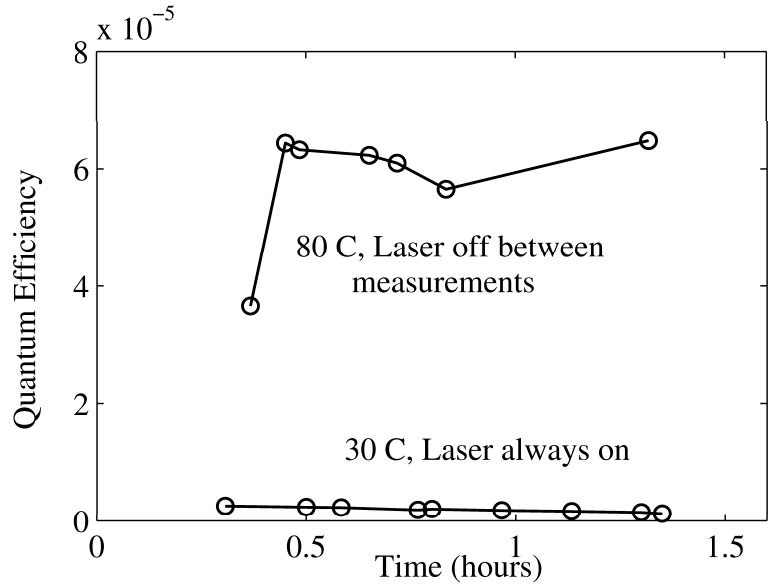

Figure 3.10: Quantum efficiency of the dispenser cathode with 532-nm light

An interesting effect is seen in figure 3.11. Here, the extracted charge is plotted versus accelerating voltage. Although the current is far below the space charge limit, it shows no sign of leveling off at higher fields due to limited emission. This means that

the influence of the Schottky effect is significant. Therefore, the work function of the cathode under these conditions must be close to the energy of the photon, 2.34 eV. In this regime, changing the temperature should also affect the quantum efficiency. More experiments will be carried out to explore these dependencies.

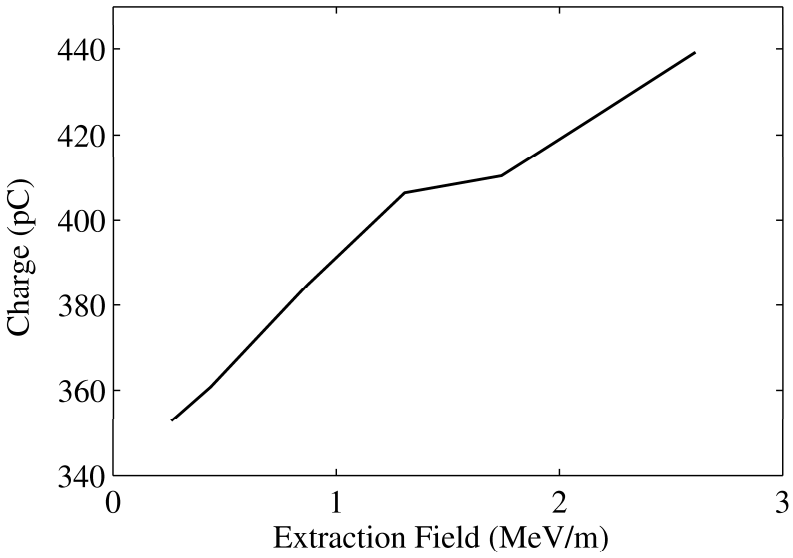

Figure 3.11: With 532-nm light, the Schottky effect is seen even at low fields

Chapter 4

Conclusions

4.1 Performance of the Cathode Test Cell

During these experiments, the cathode test cell has been shown to meet all of its performance goals. It has been shown to operate at fields of up to 10 MeV/m. The pressure in the cell is between 10^{-9} and 10^{-10} torr. In averaging mode, sub nanosecond features can be resolved. More work will be done to improve the signal fidelity in single shot mode. For a 1-cm gap, a charge of 1–2 nC can be generated before current is lost to space charge effects. The quantum efficiency measured for copper, 1×10^{-5}, is comparable to the value that others have measured.

4.2 Photoemission from the Scandate Cathode

So far, the highest quantum efficiency measured for the scandate cathode has been 8×10^{-4} with a 266-nm laser. Already, this value is one of the highest for a metal accelerator cathode measured at low fields. At 532 nm, a quantum efficiency of 6.2×10^{-5} has been recorded. Even at the fourth harmonic, copper cannot match this value. Also, because this cathode can be thermally rejuvinated, it has the same advantage of long

lifetime that copper has.

This cathode compares favorably with the known photoemission results for other thermionic cathodes. Compared to the performance of the standard B cathode [13], this cathode displayed roughly twice the quantum efficiency at each harmonic. A nitrogen laser, which has a wavelength of 337 nm, lies close to the wavelength of the third harmonic (355 nm). At 337 nm, the quantum efficiency of an older B type cathode was found to be 7.4×10^{-5}, between two and three times below that of the scandate cathode. LaB_6, another thermionic (but not dispenser) cathode which has been tested in an rf gun [17], has a quantum efficiency of up to 1×10^{-3} at 337 nm [18]. However, it must be heated to over 1000 C and sometimes cracks during use.

As expected, the cathode is sensitive to contamination. By holding the cathode at an elevated temperature, this effect can be mitigated. Also, it was noted that running the laser accelerates the poisoning process under most circumstances. However, this problem may not exist in an rf gun. In these experiments, an anode was placed directly in front of the cathode to create the dc field. Light is intercepted by the the grid, and light reflects off the cathode and hits the anode structure, which releases contaminants in close proximity to the cathode. In an rf gun, there are no surfaces near the cathode for the light to hit. Also, a dc field attracts ions to the cathode, whereas an alternating field will have no net effect on their position.

It should be noted that it has so far been impossible to make measurements for a completely clean surface. While waiting for the cathode to cool below the point where thermionic emission occurs, impurities have already begun to accumulate. By using a pulsed extraction voltage, so that some thermionic emission can be tolerated, it would be possible to make a more accurate measurement. Improving the vacuum would also allow better values to be obtained. It has been suggested that by illuminating the

system with a high power ultraviolet lamp, it may be possible to clean the anode so that there is no initial burst of contaminants when the laser is switched on. In any case, the numbers reported here represent a lower bound on the quantum efficiency for the scandate dispenser cathode.

The measurements so far have been made with accelerating fields of less than about 1 MeV/m. It is not uncommon for the quantum efficiency to increase by a few times at the fields used in rf guns. With the current arrangement, the field can be increased to 10 MeV/m. At a later stage in the project, the cathode may be installed in an rf gun, where the cathode can be studied at fields of up to 100 MeV/m.

A direct comparison between the quantum efficiency of a cathode at different wavelengths is misleading because the efficiency of the conversion process is not taken into account. Also, even if the process is perfectly efficient, the photon energy is higher at shorter wavelengths, so the number of photons is fewer. A better analysis includes these variations. Specifically, the number of electrons generated for each infrared photon can be used as the basis for the comparison. Conversion efficiencies vary from laser to laser. Here, the values for the laser used in this experiment are assumed, which can be taken as representative. Efficiencies at the second, third, and fourth harmonic are .5, .16, and .08. Table 4.2 presents the results. It shows that this cathode should be used with a 532-nm drive laser, which gives it a significant advantage over conventional metal cathodes.

4.3 Future Directions

Because of the promising results obtained for this cathode, the next step will be to test the other commercially available dispenser cathodes. The original work cited in

λ	N_γ	QE	e^- / γ_{IR}
1064	1	0	0
532	.25	$.62\times10^{-4}$	1.5×10^{-5}
355	.05	1.7×10^{-4}	$.85\times10^{-5}$
266	.02	8.0×10^{-4}	1.6×10^{-5}

Table 4.1: Efficiency normalized to available energy at each harmonic for the dispenser cathode. N_γ is the number of photons at the given wavelength generated for each original infrared photon. e^- / γ_{IR} is the number of electrons produced for each infrared photon.

Chapter 1 was based on a 4:1:1 type B cathode, and the cathode used for these experiments is a 3:1:1 scandate cathode. No 5:3:2 or 6:1:2 cathodes have been tested, and no type M (coated) cathode has been tested. A 5:0:2 cathode, which contains no calcium oxide, can also be fabricated. These cathodes may differ in quantum efficiency and lifetime.

The alkalis are the lowest work function metals. They cannot be used for thermionic emission because their melting point is too low. However, if a dispenser type cathode could be designed that maintained a monolayer of an alkali metal on a tungsten surface, high quantum efficiencies could be achieved. In this case, emission is from the substrate with enhancement due to a dipole layer. Even if the layer were thick enough so that the emission was entirely from the surface film, alkali metals have a high enough quantum efficiency in the visible spectrum that an improvement over existing metal cathodes would still be made. A dispenser cathode for lithium has already been studied [19].

Ultimately, the feasibility of a dispenser semiconductor cathode will be investigated. For instance, the cesium antimony cathode is formed by sputtering antimony

on a substrate and then exposing it to cesium vapor. Its lifetime is limited by poisoning and the loss of cesium. If the cathode were heated to drive off the contaminants, cesium loss would be accelerated. In a dispenser arrangement, the cathode could be heated, and lost cesium would be replaced from the reservoir. Such a cathode would be an ideal source for an rf gun.

Appendix A

Dynamics of Space Charge Diodes

In the experiments related to this thesis, a dc field is used between the cathode and the anode. There is a limit to the current that can be drawn through any such device. If the diode operates in the space charge limited regime, not all of the photoelectrons will be extracted, so the quantum efficiency will be underestimated. The theories below can be used to predict the regime were the emission will be source limited.

At high currents, space charge effects influence the electron dynamics in the anode–cathode region. The steady state case for a parallel plate geometry of infinite extent can be solved analytically. The equation, known as the Child-Langmuir law [20], is

$$J = \frac{4\epsilon_0}{9}\sqrt{\frac{2e}{m}}\frac{V^{\frac{3}{2}}}{d^2} \tag{A.1}$$

Photoinjectors produce pulses that are small in time and space. Consequently, the current limit predicted by equation A.1 can be greatly exceeded. The motion of the electrons can no longer be described analytically, and instabilities may develop.

Recently, a theory has been proposed that explains the limiting current in diodes of finite emitting area [21]. It determines how much current is need to generate a virtual cathode, which is a point in the gap where the potential is lower than that of the cathode. When a virtual cathode has formed, no more current can flow into the region,

so an equilibrium is reached. For the case of a circular disk of radius r, the equation is

$$J \approx (1 + \frac{d}{4r}) J_{Child} \tag{A.2}$$

where the assumption is made that $r/d \gg 1$. The theory agrees with the results from detailed computer simulations.

Another theory describes the behavior of a diode of infinite extent in the case where the pulse is short compared to the gap spacing [16]. Importantly, for this case it was found that the total charge that can be drawn is relatively invariant to pulse length. The exact expression is

$$J \approx 2 \frac{1 - \sqrt{1 - \frac{3}{4}(\frac{\tau_p}{T_{CL}})^2}}{(\frac{\tau_p}{T_{CL}})^3} J_{Child} \tag{A.3}$$

where τ_p is the pulse length and

$$T_{CL} = 3D\sqrt{\frac{m}{2qV}} \tag{A.4}$$

is the transit time of an electron under the conditions assumed for the Child-Langmuir law.

Appendix B

University of Maryland Electron Ring

The University of Maryland Electron Ring (UMER) [22] is used to study space charge dominated beams. The gun uses a gridded thermionic cathode and a 10 kV dc field to produce 70 ns, 100 mA beams. For most purposes, the beam is long enough that it can be considered two dimensional. As part of the research reported here, a laser will be used to produce short bursts of electrons independently from or in addition to the thermionic beam. This will expand the possibilities for studying longitudinal dynamics. It will also be possible to perturb the beam with complete spatial and timing freedom. In support of this research, a retractable mirror system has been inserted into the beam pipe so that a laser can be aimed at the cathode.

Because UMER is devoted entirely to beam physics, it has diagnostics capable of measuring a broad range of beam parameters. There is a fluorescent screen and a capacitive pickup beam position monitor (BPM) in 14 chambers distributed around the ring. Additionally, the beam can be extracted into a diagnostic chamber that houses an energy analyzer, a slit-slit emittance meter, and a pepper pot.

The phosphor screens have a millisecond response time, so they are capable of measuring the transverse distribution of total charge. The spatial resolution is about .5 mm. The BPMs can follow a rise time of 1.5 ns, so they will be capable of re-

solving the laser induced emission. The information they provide is centroid position, longitudinal current distribution, and some transverse distribution data.

The energy analyzer has a rise time of about 10 ns, so it will only be able to provide time integrated values. Its spatial resolution is determined by the aperture size, which is 2 mm. The slit-slit system has a response time similar to that of the BPM. The width of the collector slit is 20 mil.

BIBLIOGRAPHY

[1] R.L. Sheffield et al. RF photoelectron gun experimental performance. In *Proc. 1998 Linear Accelerator Conf.*, pages 520–522, 1988.

[2] R.L. Sheffield. High brightness electron sources. In *Proc. 1995 Particle Accelerator Conf.*, pages 882–886, 1996.

[3] S.H. Kong et al. Photocathodes for free electron lasers. *Nucl. Instrum. and Methods*, A358:272–275, 1995.

[4] W.E. Spicer and A. Herrera-Gomez. Modern theory and applications of photocathodes. In *Proc. SPIE*, volume 2022, pages 18–33, 1993.

[5] M. Cardona and L. Ley. *Photoemission in Solids I*, pages 105–134. Springer-Verlag, New York, 1978.

[6] C. Herring and M.H. Nichols. Thermionic emission. *Rev. Mod. Phys.*, 21(2):185–270, 1949.

[7] R.H. Fowler. The analysis of photoelectric sensitivity curves for clean metals at various temperatures. *Phys. Rev.*, 38:45–56, 1931.

[8] S.H. Kong et al. Fabrication and characterization of cesium telluride photocathodes: A promising electron source for the Los Alamos Advanced FEL. *Nucl. Instrum. Methods*, A 358:276–279, 1995.

[9] N.D. Lang. Theory of work-function changes induced by alkali adsorption. *Phy. Rev. B*, 4(12):272–275, 1971.

[10] R.L. Bell. *Negative Electron Affinity Devices*, pages 1–5. Claredon Press, Oxford, 1973.

[11] J.L. Cronin. Modern dispenser cathodes. *Proc. IEE*, 128(1):19–32, 1981.

[12] R.E. Thomas et al. Thermionic sources for high-brightness electron beams. *IEEE Trans. Electron Devices*, 37(3):853–861, 1989.

[13] B. Leblond. Short pulse photoemission from a dispenser cathode under the 2nd, 3rd and 4th harmonics of a picosecond Nd:YAG laser. *Nucl. Instrum. Methods*, A317:365–372, 1991.

[14] D.W. Feldman et al. Combined thermionic and photoelectric emission from dispenser cathodes. In *Proc. 2001 Particle Accelerator Conf.*, pages 2132–2134, 2001.

[15] C. Travier et al. Candela photo-injector experimental results with a dispenser cathode. In *Proc. 1995 Particle Accelerator Conf.*, volume 2, pages 945–947, 1996.

[16] A. Valfells et al. Effects of pulse-length and emitter area on virtual cathode formation in electron guns. *Phys. Plasmas*, 9(2):2377–2382, 2002.

[17] P.G. O'Shea et al. Radio frequency photoinjector using LaB_6 cathode and a nitrogen laser. *Appl. Phys. Letters*, 73(3):411–413, 1998.

[18] M.H. Bakshi D.J. Bamford and D.A.G. Deacon. The search for rugged, efficient photocathode materials. *Nucl. Instrum. Methods*, A 318(1-3):377–380, 1992.

[19] A. Septier et al. A binary Al/Li alloy as a new material for the realization of high-intensity pulsed photocathodes. *Nucl. Instrum. Methods*, A 304:392–395, 1991.

[20] M. Reiser. *Theory and Design of Charged Particle Beams*, pages 45–46. John Wiley & Sons, Inc., New York, 1994.

[21] Y.Y. Lau. Simple theory for the two-dimensional Child-Langmuir law. *Phys. Rev. Letters*, 87(27), 2001.

[22] P.G. O'Shea et al. UMER: The University of Maryland Electron Ring. *Nucl. Instrum. Methods*, A 464(1-3):646–652, 2002.